

1-1-2000

Deconstructing the interaction of glu-plasminogen with its receptor a-enolase

N M. Andronicos
University of Wollongong

M S. Baker
University of Melbourne

M Lackmann
Royal Melbourne Hospital, Parkville, Victoria, Australia

M Ranson
University of Wollongong, mranson@uow.edu.au

Follow this and additional works at: <https://ro.uow.edu.au/scipapers>



Part of the [Life Sciences Commons](#), [Physical Sciences and Mathematics Commons](#), and the [Social and Behavioral Sciences Commons](#)

Recommended Citation

Andronicos, N M.; Baker, M S.; Lackmann, M; and Ranson, M: Deconstructing the interaction of glu-plasminogen with its receptor a-enolase 2000, 327-336.
<https://ro.uow.edu.au/scipapers/4257>

Deconstructing the interaction of glu-plasminogen with its receptor a-enolase

Keywords

receptor, its, plasminogen, glu, interaction, enolase, deconstructing

Disciplines

Life Sciences | Physical Sciences and Mathematics | Social and Behavioral Sciences

Publication Details

Andronicos, N. M., Baker, M. S., Lackmann, M. & Ranson, M. (2000). Deconstructing the interaction of glu-plasminogen with its receptor a-enolase. *Fibrinolysis & Proteolysis*, 14 (6), 327-336.

Deconstructing the interaction of glu-plasminogen with its receptor α -enolase

N. M. Andronicos¹, M. S. Baker², M. Lackmann³, M. Ranson¹

¹Department of Biological Sciences, University of Wollongong, NSW, 2522, Australia ²Gynaecological Cancer Research Centre and Department of Obstetrics and Gynaecology, University of Melbourne, Royal Women's Hospital, Carlton, Victoria, Australia ³Ludwig Institute for Cancer Research, Royal Melbourne Hospital, Parkville, Victoria, Australia

Summary Objective: Plasminogen binds with apparent low-affinity to cell-surface receptors via its lysine binding sites. This enhances/stabilizes the activation-susceptible conformation. However, it is not known whether this lysine-mediated conformational change of plasminogen may affect its subsequent dissociation rate and hence its stability at the cell surface. Therefore, we sought to determine the relationship between the lysine-dependent conformation of plasminogen and its dissociation rate from its receptor.

Design: BIACORE experiments were used to determine the kinetics of the interaction of glu-plasminogen with its receptor α -enolase. Intrinsic and extrinsic fluorescence spectroscopy were utilized to confirm if α -enolase induced a conformational change to glu-plasminogen as predicted by analyses of the BIACORE data.

Results: The dissociation of glu-plasminogen from α -enolase was mediated by at least two components with apparent dissociation rate constants of $k_{d1} = 4.7 \times 10^{-2} \text{ s}^{-1}$ and $k_{d2} = 1.6 \times 10^{-3} \text{ s}^{-1}$. This second slower dissociation event reflects an increase in the stability of the complex. Global analysis of the interaction suggested a two-state conformational change reaction, mediated by a concentration-dependent increase in the initial association rate constant. The apparent K_d predicted by this analysis was $1 \mu\text{M}$. Fluorescence spectroscopy confirmed that α -enolase induced a more open conformation of glu-plasminogen.

Conclusions: These results provide direct evidence that the binding of glu-plasminogen to α -enolase is not simply a low-affinity interaction, but involves a multivalent, competition binding reaction that is associated with a glu-plasminogen conformational change. This mechanism is compatible with the structure of glu-plasminogen. This has implications for the stability of binding and activation of glu-plasminogen at the cell surface. © 2000 Harcourt Publishers Ltd

INTRODUCTION

Plasmin is responsible for a wide variety of physiological and pathological processes which involve the breakdown of tissue barriers and cell migration. Plasmin, a trypsin-like broad spectrum serine endopeptidase, is generated from the zymogen glu-plasminogen (glu-plg) which is abundant (present at approximately $2 \mu\text{M}$) in plasma.¹ Human glu-plg¹ (EC 3.4.21.7) is a single chain 790 amino-acid glycoprotein that has an apparent molecular weight of 92 kDa.¹ Glu-plg is composed of both a

heavy chain (65 kDa), containing the N-terminal peptide (NTP) and five triple-disulfide-bonded kringle (K) domains, and a light chain (25 kDa) or protease domain chain.¹ The crystal structures of the individual K1,² K4^{3,4} and K5⁵ of plg have been solved and demonstrate that the lysine binding site (LBS) motifs are pre-formed and localized to the surfaces of the kringle domains. Glu-plg exhibits a closed, right-handed, spiral conformation.^{6–8} Removal of NTP from glu-plg results in the formation of lys-plg (86 kDa)⁹ which has a more open, U-shaped conformation than glu-plg.^{10,11}

Site-directed mutagenesis studies, which removed the lysine binding function of individual kringle domains, have demonstrated that the closed conformation of glu-plg is maintained by the binding of multiple kringle LBS motifs with internal lysine residues^{12,13} such as Lys₅₀ and

Received: 26 July 2000

Accepted: 26 July 2000

Correspondence to: Nicholas M. Andronicos, Dept. Biological Sciences, University of Wollongong, Wollongong NSW 2522, Australia.
Tel.: +61 2 4221 4356; fax: +61 2 4221 4135; e-mail: nma01@uow.edu.au

Lys₆₂ located in the NTP of glu-plg.¹³ The presence of this intramolecular lysine-binding network suggests the LBS motifs of glu-plg are occupied by the internal lysine residues of the protein. Disruptions to the intramolecular lysine binding network of glu-plg by exogenous lysine analogues induces an open conformation of glu-plg. The interactions of lysine analogues at multiple sites within glu-plg change the conformation of the protein from its closed to open state.^{14,15} This conversion is not accompanied by a change in the secondary structure of glu-plg,^{16,17} but is dependent upon the interactions of the kringle domains with lysine residues. Christensen and Molgaard¹⁸ demonstrated that a rapid conformational change of glu-plg ($t_{1/2} = 0.01$ s) is mediated by the cooperative binding of the LBS motifs of K5 and K4 to the small lysine analogue ϵ -amino caproic acid (ϵ -ACA).¹⁹ Marshall et al.¹⁰ suggested that glu-plg can actually exist in three distinct conformations in vitro; α (closed), β (partially open), and γ (fully open). Incubation of glu-plg α with the K5 specific ligand, benzamidine,²⁰ induces the formation of glu-plg β .¹⁰ Subsequent treatment of glu-plg β with ϵ -ACA induces the formation of glu-plg γ ,¹⁰ confirming that the cooperative interaction between K5 and another LBS is responsible for inducing the fully open conformation of glu-plg.

The binding of small lysine analogues to glu-plg changes the conformation to a form that is susceptible to activation by the plg activators.^{14,15,21–23} The activation of glu-plg is also enhanced by a lysine-dependent interaction with macromolecules such as fibrin,²⁴ various cell types,^{25,26} and isolated cellular plg receptors such as α -enolase.^{27,28} Several studies, including our own,^{26,27} have utilized various end-point assays to study the interaction of glu-plg with both cells and cellular plg receptor molecules.^{27,28} These studies have provided information on binding parameters such as affinity and binding capacity (in the case of intact cells), however, the type of binding kinetics of glu-plg have not been determined. We, therefore, used BIACORE technology to characterize in real-time the relationship between binding and conformational switching of glu-plg using recombinant α -enolase as a model receptor.²⁷ Furthermore, fluorescence spectroscopy was used to confirm α -enolase-induced conformational changes in glu-plg observed by BIACORE analysis. In addition, we attempted to analyze the type of binding kinetics lys-plg undergoes using BIACORE technology under identical conditions to those used for glu-plg. We reasoned that since lys-plg has a more open conformation than glu-plg,^{10,11} by comparing the binding kinetics between the two plg forms, we would gain additional insights into the binding mechanism of glu-plg. The results presented here provide direct evidence that the binding of glu-plg to α -enolase involves a multivalent, competition binding reaction that is associated with a conformational change in glu-plg.

The implications of these data will be discussed in terms of the activation of glu-plg.

MATERIAL AND METHODS

Recombinant human hexa-histidine-tagged α -enolase was purified as previously described²⁷ and will be referred to as α -enolase throughout the text. Human plasmin, glu- and lys-plg were generous gifts from Dr Richard Hart, American Diagnostica Inc. (Greenwich, CT, USA). Glu-plg was labelled with fluorescein isothiocyanate (FITC) as described previously.²⁶

BIACORE binding assays

The binding of glu-plg to recombinant α -enolase was analyzed on the BIACORE optical biosensor (Pharmacia Biosensor, Sweden) using either α -enolase-(His)₆-derivatized CM 5 or NTA-modified sensor chips. Covalent immobilization of α -enolase onto N-hydroxysuccinimide (NHS, 0.05 M)/N-hydroxysuccinimide-N-ethyl-N'-(diethylaminopropyl)carbodiimide (0.2 M) – activated sensor chips was performed essentially as described.²⁹ Prior to analysis, plg was buffer exchanged (Phast-desalting column, 100 × 3.2 mm, Amersham-Pharmacia) into BIACORE running buffer (10 mM Hepes, 150 mM NaCl, 1.4 mM EDTA, 0.005% Tween-20, pH 7.4) and adjusted to a concentration of 10 μ M. From this stock solution, dilutions were prepared for BIACORE experiments. The affinity surface was regenerated between subsequent sample injections of plg with 35 μ l of a desorption buffer (3 M MgCl₂, 0.075 M Hepes/NaOH, 25% ethylene glycol, pH 7.2) followed by two washes with BIACORE running buffer. α -enolase (His)₆ (15 μ l, 200 nM) was also bound onto a NTA-modified sensor chip (BIACORE AB, Sweden) which had been charged with an injection of 25 μ l NiCl₂ (0.5 mM) in modified running buffer containing 50 μ M EDTA. In these experiments the chip surface was regenerated after sample application by sequential 15 μ l-injections of 6 M guanidine-hydrochloride, 50 mM EDTA, 20 mM Tris-HCl (pH 8.6) and of 0.35 M EDTA, 0.15 M NaCl, 0.005% Tween 20 (pH 8.2). To minimize differences in the α -enolase concentration on the chip surface, injection of both NiCl₂ and α -enolase (His)₆ from the same NiCl₂ and α -enolase stock solutions were used for all experiments.

Analysis of BIACORE sensorgram data

BIACORE sensorgram data were fitted as described previously³⁰ to the reaction models included in the BIAevaluation software. Briefly, a minimum of six data sets corresponding to plg binding reactions at concentrations between 4 μ M and 63.5 nM were analyzed. Fitting the

sensorgram data to the algorithms of reaction schemes 1 and 2 involved analyzing the individual association or dissociation phases of each binding reaction using the BIAevaluation software, version 3.0. The global fit modeling of reaction schemes 3–5 involved the simultaneous fitting of the association and dissociation phases of the individual binding reactions.

Both the χ^2 -statistical test and the distribution of the residuals were used to determine whether a particular reaction scheme was a good mathematical representation of the plg binding sensorgram data. Theoretical models that displayed small χ^2 values and which did not vary by a large magnitude over the range of plg concentrations examined, were deemed to be a good mathematical representation of the sensorgram data. Deviations of the sensorgram data from a theoretical reaction scheme model that had small χ^2 statistics had to also have small and random deviation from the sensorgram data (residuals), since the magnitude and distribution of these residuals demonstrates the quality of the sensorgram data.

Reaction scheme 1

- $A + B \leftrightarrow AB$: a simple 1 : 1 Langmuir kinetic.

Reaction scheme 2

- $A_i + B_i \leftrightarrow A_i B_i$: a two or more component dissociation kinetic model, confined to the estimation of the dissociation rates for each of the components of the interaction since knowledge of the analyte (plg) concentrations that contribute to its interaction with ligand (α -enolase) are not required.

Reaction scheme 3

- $A + B \leftrightarrow AB \leftrightarrow A^*B$: the two-state reaction/conformational change model – analyte ($A = \text{plg}$) binds to ligand ($B = \alpha$ -enolase). Complex AB changes to A^*B which cannot dissociate directly to $A + B$ without first undergoing the reverse conformational change.

Reaction scheme 4

- $A + B_1 \leftrightarrow AB_1$; $A + B_2 \leftrightarrow AB_2$: heterogeneous ligand ($B = \alpha$ -enolase), parallel interactions – one analyte ($A = \text{plg}$) binds independently to two ligand binding sites (B_1, B_2). Two independent sets of rate constants, k_{a1}, k_{d1} and k_{a2}, k_{d2} .

Reaction scheme 5

- $A + B \leftrightarrow AB$; $AB + B \leftrightarrow AB_2$: bivalent analyte A (plg) binds to a monovalent ligand B (α -enolase).

Intrinsic fluorescence spectroscopy

All fluorescence experiments were performed using a F4500 Fluorimeter (Hitachi) with a slit width of 5 nm at

room temperature. Plg species ($1 \mu\text{M}$) in 50 mM Tris-HCl (pH 7.0), 100 mM NaCl were excited at 280 nm and the intrinsic fluorescence emission spectra were measured from 300–450 nm.

Extrinsic fluorescence spectroscopy

All FITC-plg fluorescence studies were performed using a Biolumin 960 (Molecular Dynamics) fluorescent plate reader equipped with a FITC set of filters (excitation: 480 ± 10 nm; emission: 520 ± 10 nm). FITC-glu-plg ($10 \mu\text{g/ml}$) in 50 mM Tris-HCl (pH 7.2), 150 mM NaCl was incubated with various concentrations of either tranexamic acid (0–20 mM), poly-D-lysine (0–2.5 mg/ml) or α -enolase (0–40 $\mu\text{g/ml}$) in a total volume of 200 μl for 5 min in the dark at room temperature. The fluorescence intensity data were normalized by calculating the change in fluorescence percentage of FITC-glu-plg ($\Delta F\%$). The fractional saturation (y) was calculated using the equation: $(F - F_i)/(F_f - F_i)$, where F_i is the initial fluorescence of FITC-glu-plg in the absence of ligand, F_f is the fluorescence of FITC-glu-plg at the maximal ligand concentration used and F is the fluorescence associated with a specific concentration of ligand.

RESULTS

Dissociation kinetics of glu- and lys-plg from immobilized α -enolase

This study describes for the first time the dissociation kinetics of glu- and lys-plg from sensor chip-immobilized α -enolase. The BIACORE sensorgrams (binding curves) obtained from the binding of increasing concentrations of glu- and lys-plg to NHS-immobilized α -enolase are shown in Figure 1. A qualitative assessment of the sensorgrams reveals obvious differences in the interaction of glu-plg (Fig. 1A) and lys-plg (Fig. 1B) binding with α -enolase. This was most evident in the contours of their apparent steady-state phases (between arrow I and II) which did not result in equilibrium binding under these experimental conditions. Importantly, the contour of the sensorgrams suggested a heterogeneous interaction for both glu- and lys-plg with α -enolase.

By comparing the fit of the experimental data to different kinetic algorithms available in the BIAevaluation software, we set out to establish a suitable kinetic model for the observed binding data (Table 1). The linear one-to-one pseudo-first order model (Reaction scheme 1) did not fit the data, as indicated by a pronounced decrease in the 'goodness of fit' χ^2 (increase of χ^2 above the 'signal noise' of 3 – 6 RU) with increasing plg concentrations (Table 1), and by a marked deviation of the 'offset values' (deviation of the fitted response at $t = \infty$) from zero

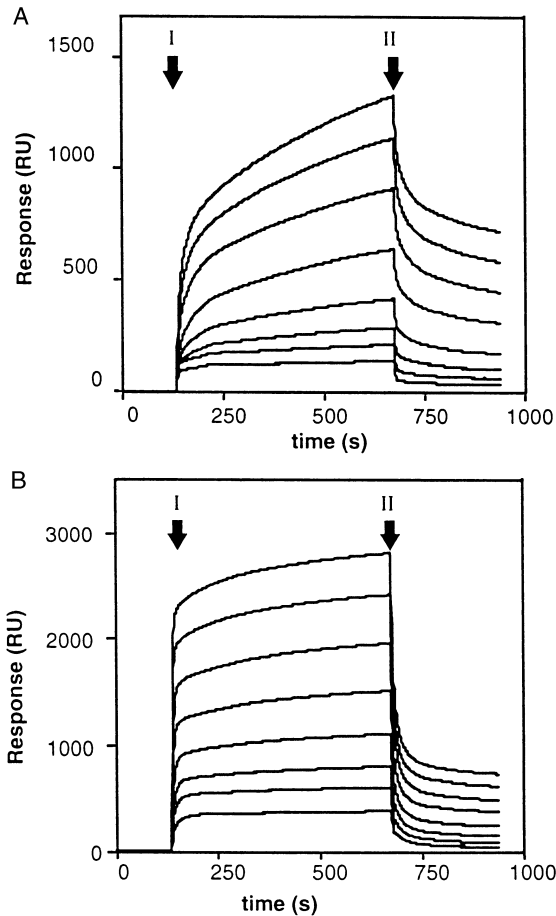


Fig. 1 BIAcore analysis of glu- and lys-plg binding to NHS-immobilized α -enolase. (A) Samples containing increasing concentrations of glu-plg in BIAcore running buffer were injected onto a sensor chip which had been derivatized with immobilized α -enolase using NHS/EDC chemistry. The decreasing responses reflect samples containing 4, 3, 2, 1, 0.5, 0.25, 0.125, 0.0625 μ M glu-plg. Arrows marked with I and II indicate the start and end of the sample injection (start of association and dissociation phases) respectively. (B) The response curves for the interaction of varying concentrations of lys-plg with the sensorchip-immobilized α -enolase are shown. Coupling of α -enolase and concentration of lys-plg were according to the conditions described in A.

(not shown). Similarly, the concentration-dependent increase of χ^2 values in the fit of association data to the single component model confirms that the interaction cannot be described adequately by this model. In contrast, the multiple component dissociation model (reaction scheme 2), which does not require knowledge of the concentration of plg, produced an accurate fit to the dissociation data and yielded χ^2 values close to zero (Table 1) as well as small random residuals for all concentrations of glu- and lys-plg analyzed. Statistical comparison of the fits (χ^2 values) to the two models by F-test confirmed that the multiple component model is a better mathematical representation of these data, since F-test values

of 1.0 were obtained for both glu- and lys-plg binding. Thus, the dissociation of glu- and lys-plg from α -enolase was mediated by at least two reactions.

Both glu- and lys-plg had similar, apparently rapid (low affinity) dissociation rate constants ($k_{d1} = 4.7 \times 10^{-2} \text{ s}^{-1}$ and $4.0 \times 10^{-2} \text{ s}^{-1}$ respectively) from NHS-immobilized α -enolase (Table 1). While the slow dissociation rate constant (higher affinity) component of lys-plg ($k_{d2} = 6.3 \times 10^{-4} \text{ s}^{-1}$) was twofold lower compared to that of glu-plg ($k_{d2} = 1.6 \times 10^{-3} \text{ s}^{-1}$) (Table 1), it was clear that both glu- and lys-plg interacted with α -enolase via at least two distinct binding sites. In addition, ϵ -ACA competitively disrupted the binding of glu- and lys-plg to NHS-immobilized α -enolase (data not shown), confirming the role of lysine in these interactions.^{27,28} Similar binding experiments were also performed using a sensor chip with substantially less NHS-immobilized α -enolase (1.3 ng/mm² versus 4.3 ng/mm² immobilized). Whilst the overall responses were reduced, very similar binding characteristics were observed (data not shown). This indicated that the kinetics were not effected by mass-transfer limitations during the interactions of glu- and lys-plg on the more densely derivatized sensor chip.

The kinetics of the interaction between plg and α -enolase were also analyzed using α -enolase that was immobilized in a defined orientation via its N-terminal 6-Histidine tag. This was done to determine if the random orientation of α -enolase contributed to the multiple component kinetics of the interaction. Sensorgram binding curves, similar to those reported in ure 1, were observed for both glu- and lys-plg binding, and a representative set of glu-plg sensorgrams are shown in Figure 2. The estimated dissociation rate constants ($k_{d1} = 6.1 \times 10^{-2} \text{ s}^{-1}$ and $k_{d2} = 1 \times 10^{-3} \text{ s}^{-1}$) were also comparable to those obtained for the binding of glu-plg to NHS-immobilized α -enolase (Table 1). Thus, the multiple component dissociation reaction model (Reaction scheme 2) best approximated the dissociation phase of glu- and lys-plg interaction with α -enolase.

Global fitting of the plg/ α -enolase binding data

Global fitting of the BIAcore binding data was performed in order to further define the interaction mechanisms. The entire binding data describing the plg/ α -enolase interaction at different plg concentrations were fitted to a number of kinetic algorithms, including linear one-to-one interaction and several complex interaction models. The selected kinetic model(s) were then used to simultaneously analyze the kinetic parameters of the association and dissociation phases of the individual plg/ α -enolase binding curves (Tables 2 & 3). The probability of an appropriate fit of the experimental data to the selected model are also shown in Tables 2 and 3.

Table 1 Kinetic analysis of the interaction of glu-plg with α -enolase from the BIACORE sensorgrams

Experiment	Kinetic constants Single component ($A + B \leftrightarrow AB$) ¹		Kinetic constants Single component ($A_i + B_i \leftrightarrow A_i B_i$) ²	
	k_a ($M^{-1}s^{-1}$)	k_d (s^{-1})	k_{d1} (s^{-1})	k_{d2} (s^{-1})
Glu-Plasminogen (NHS ³) (goodness of fit (χ^2))	2.8×10^4 (0.054–7.51)	3.2×10^{-3} (0.073–88.2)	4.7×10^{-2} (0.0203–0.060)	1.6×10^{-3} (0.0389–0.112)
Lys-Plasminogen (NHS ³) (goodness of fit (χ^2))	3.4×10^5 (0.088–7.35)	4.0×10^{-3} (3.29–83.2)	4.0×10^{-2} (0.0389–0.112)	6.3×10^{-4} (0.0389–0.112)
Glu-Plasminogen (NTA ⁴) (goodness of fit (χ^2))	4.1×10^4 (0.05–15.8)	1.4×10^{-3} (0.102–13.7)	6.1×10^{-2} (0.015–0.061)	1.0×10^{-3} (0.015–0.061)

¹ Association and dissociation rate constants derived from progress data of the BIACORE sensorgrams using linear kinetic models included in the BIAevaluation software, $R = R_{eq}(1 - e^{-(k_a C + k_d)(t - t_0)})$, where R_{eq} is the steady state response (R) which is not necessarily reached in the sensorgram, C = molar concentration, t_0 = start time of sensorgram. The time interval for the analysis of the association rate constants were 138 s–165 s (Figs 1 & 2). The time interval for the analysis of the dissociation rate constants were 695 s–750 s (Figs 1 & 2).

² Dissociation rate constants for two parallel dissociation reactions were estimated according to $R = R_1 e^{-k_{d1}(t-t_0)} + (R_0 - R_1) e^{-k_{d2}(t-t_0)}$, where R_1 and $R_0 - R_1$ are the contributions to R_0 from component 1 and 2 respectively (Figs 1 & 2).

³ Experiments on a CM-5 sensor chip derivatized with enolase using NHS/EDC chemistry to yield an increase in the baseline response of 3900 RU. Following each cycle the chip surface was regenerated by desorption of non-covalently bound protein with a $MgCl_2$ /ethylene glycol buffer (see methods) (Fig. 1).

⁴ Experiments on a Ni-NTA-derivatized sensor chip carrying α -enolase coupled by its N-terminal 6-his affinity tag to yield an increase of 1800 RU above baseline. Following each cycle α -enolase together with the Ni^{2+} was stripped from the NTA-chip with $GnHCl/EDTA$ (see methods) and the chip re-charged with Ni^{2+} and loaded with α -enolase (Fig. 2).

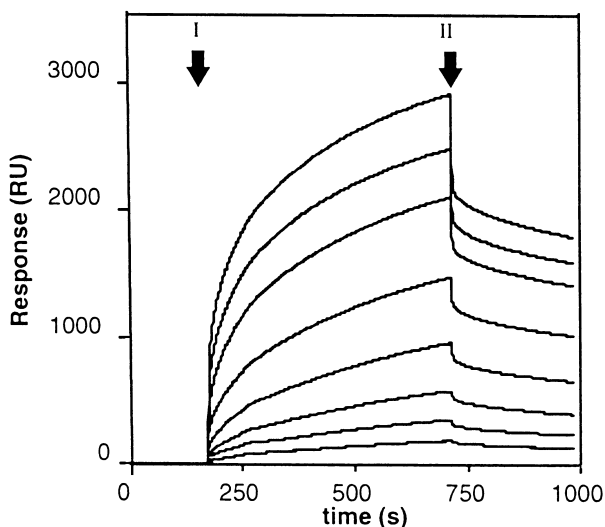


Fig. 2 BIACORE analysis of glu-plg binding to Ni^{2+} -NTA immobilized α -enolase. α -enolase was immobilized onto a Ni^{2+} -NTA chip by its N-terminal 6-his affinity tag. The decreasing responses reflect samples containing 4, 3, 2, 1, 0.5, 0.25, 0.125 and 0.0625 μ M glu-plg. Following each injection of glu-plg, bound ligand, Ni^{2+} and α -enolase were stripped from the Ni^{2+} -NTA-chip and the affinity surface regenerated by the injection of Ni^{2+} and α -enolase prior to the injection of glu-plg (see methods). The sensorgrams presented only show the progress data for the injection of glu-plg (arrow I) and its dissociation (arrow II) from the α -enolase surface.

The two-state reaction/conformational change model (Reaction scheme 3) yielded a good fit within the range of glu-plg concentrations examined (χ^2 : 0.9–2.2; Table 2;

small random residuals). As suggested by the contour of the binding curves, the interaction of glu-plg with α -enolase was characterized by an initial apparent fast dissociation rate constant ($k_{d1} = 2.64 \pm 0.6 \times 10^{-2} s^{-1}$) and an association rate constant which was increasing with decreasing glu-plg concentrations ($k_{a1} = 4.3 - 19.3 \times 10^3 M^{-1} s^{-1}$). In contrast, the second phase of the interaction appeared to proceed in a largely concentration-independent manner with markedly lower on and off rates ($k_{a2} = 3.8 \times 10^{-3} M^{-1} s^{-1}$ and $k_{d2} = 7.4 \pm 0.27 \times 10^{-4} s^{-1}$). Overall, the dissociation rate constants, derived by fitting the glu-plg binding data to this model (Reaction scheme 3), were comparable to the rate constants estimated by the multiple component dissociation reaction (Reaction scheme 2) discussed earlier (Table 1). Furthermore, the apparent K_d (Table 2) are comparable to the values derived using other techniques.^{27,28} Thus, the interaction of glu-plg with α -enolase may result in a conformational change to glu-plg such that it cannot dissociate from α -enolase without undergoing another conformational change.

An alternative model, assuming a heterogeneous population of sensor chip-immobilized α -enolase binding glu-plg in parallel reactions (Reaction scheme 4) yielded a markedly decreased fit with χ^2 values between 1.9 and 141 (Table 2). Thus, the heterogeneous α -enolase reaction model (Reaction scheme 4) did not adequately represent the data. Similarly, global analysis with an algorithm which adjusts for mass transfer limitations of the analyte (plg) binding to a sensor surface of high ligand

Table 2 Kinetic parameters of the glu-plg/ α -enolase interaction

Concentration μM	K_d μM	K_{a1} $\text{M}^{-1}\text{s}^{-1}$ (10^{-3})	K_{d1} s^{-1} (10^{-2})	K_{a2} $\text{M}^{-1}\text{s}^{-1}$ (10^{-3})	K_{d2} s^{-1} (10^{-4})	χ^2 Two-state-reaction ¹	χ^2 Heterogeneous ligand ¹
4	1.5	4.3	3.5	4.5	8.0	2.0	141
3	1.4	5.0	3.26	4.3	9.3	2.2	22.1
2	1.05	6.3	2.8	4.1	9.7	2.0	26.5
1	0.6	8.6	2.2	4.2	9.6	1.1	23.9
0.5	1.5	11.9	2.0	2.8	2.6	0.9	4.94
0.25	0.2	19.3	2.1	2.6	5	0.9	1.9
Mean ²	1.0		2.64	3.8	7.4		

¹ The binding data were fitted to the two kinetic algorithms of the BIAevaluation 3.0 software (see methods) which yielded the closest match of experimental data with the chosen model. The listed kinetic constants are derived in each case only from the candidate model with the closest fit (lowest χ^2 value).

² Mean values were estimated only for those parameters which did not indicate a concentration-dependent change.

Table 3 Kinetic parameters of the lys-plg/ α -enolase interaction

Concentration μM	K_d μM	K_{a1} $\text{M}^{-1}\text{s}^{-1}$ (10^4)	K_{d1} s^{-1} (10^{-2})	K_{a2} $\text{M}^{-1}\text{s}^{-1}$ (10^{-3})	K_{d2} s^{-1} (10^{-3})	χ^2 Two-state-reaction ¹	χ^2 Bivalent analyte ¹
4	3.2	2.0	7.6	3.3×10^{-3}	2.7	48.3	121
3	2.6	2.4	7.6	3.2×10^{-3}	2.6	24.7	475
2	0.8	2.6	6.6	2.6×10^{-3}	0.9	15.8	112
1	0.9	3.8	5.5	1.8×10^{-3}	1.2	41.1	1240
0.5	K_{d1} : 3.5	1.9	6.6	6.6×10^{-7}	1.1	363	8.79
0.25	K_{d1} : 1.9	2.7	5.3	7.8×10^{-7}	1.0	320	3.42
0.125	K_{d1} : 0.8	5.9	4.5	19.5×10^{-7}	1.2	193	1.96

¹ The binding data were fitted to the two kinetic algorithms of the BIAevaluation 3.0 software (see methods) which yielded the closest match of experimental data with the chosen model. The listed kinetic constants are derived in each case only from the candidate model with the closest fit (lowest χ^2 value).

(i.e. α -enolase) concentration resulted in a poor fit to the glu-plg sensorgram data (data not shown), confirming that these effects did not influence the kinetics of the interaction.

In contrast to glu-plg, the generally large χ^2 values obtained for the lys-plg binding data indicated that none of the global fitting models currently available fitted the data over the entire lys-plg concentration range used (Table 3). As stated above, the multiple component model (Reaction scheme 2) is determined independently of the association phases and provided a strong fit of the lys-plg dissociation data (Table 1). Since the dissociation rate constants shown in Table 3 were similar to those obtained by the multiple component model (Reaction scheme 2) for the same range of lys-plg concentrations (Table 1), it is possible that the association phase is the component of the binding interaction that cannot be deconvoluted by any of the global fitting algorithms currently available, at least under the physiological-like conditions used in these experiments. In any case, it is clear that glu- and lys-plg have different binding mechanisms with respect to α -enolase.

Intrinsic fluorescence spectroscopy

To qualitatively confirm that binding with α -enolase induces a conformational change in glu-plg, the intrinsic fluorescence spectra of glu-plg in the presence and absence of α -enolase were determined (Fig. 3). These were compared to the intrinsic fluorescence spectra of glu-plg in the presence and absence of the lysine analogue ϵ -ACA, previously shown to 'open' glu-plg resulting in an increase in its intrinsic fluorescence.¹⁹ In addition, the spectra of plasmin and lys-plg, which have a more open conformation than glu-plg,^{10,11} are shown for comparison.

Plasmin and lys-plg had comparable relative intrinsic fluorescence emission maxima at 330 nm (4850 and 4694 respectively). In contrast, the relative intrinsic fluorescence maximum for glu-plg was significantly lower (3480). Addition of ϵ -ACA to glu-plg (Fig. 3A) resulted in an increase in the relative intrinsic fluorescence of glu-plg ($\Delta F = 1019$) to one which was comparable to the relative fluorescence obtained for the same concentration of either lys-plg or plasmin. The addition of α -enolase to

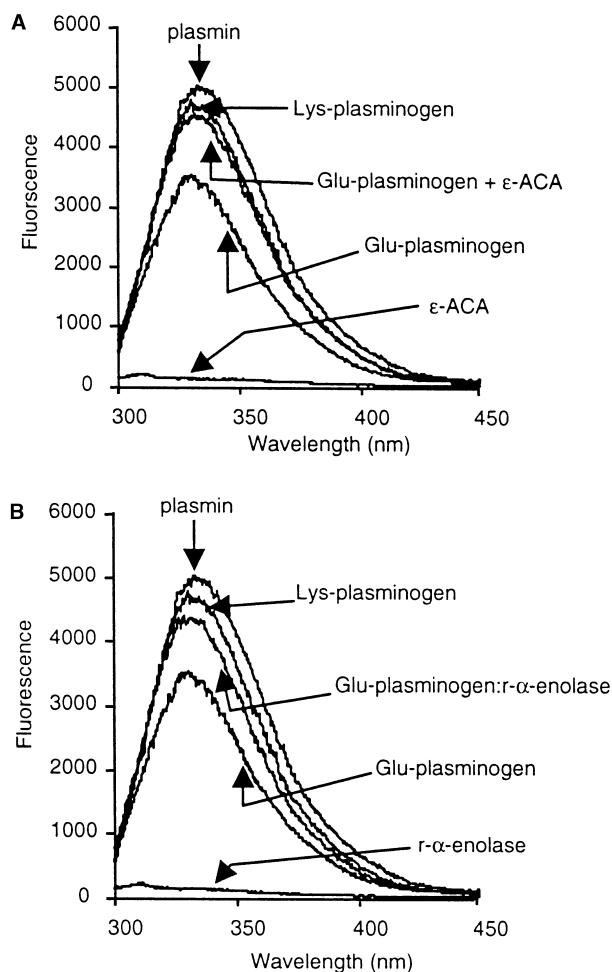


Fig. 3 Comparison of the intrinsic fluorescence spectra of glu-plg in the absence and presence of ϵ -ACA or α -enolase to those of plasmin and lys-plg. (A) The fluorescence spectra of $1 \mu\text{M}$ plasmin, glu- and lys-plg, glu-plg + 100 mM ϵ -ACA and 100 mM ϵ -ACA control were obtained after excitation at 280 nm . (B) The fluorescence spectra of $1 \mu\text{M}$ plasmin, glu- and lys-plg, glu-plg + 190 nM α -enolase and 190 nM α -enolase control were obtained after excitation at 280 nm . The intrinsic fluorescence spectra of both ϵ -ACA (117) and α -enolase (146) at the concentrations used for these experiments were negligible. Higher concentrations of α -enolase could not be used as this alone was associated with increased intrinsic fluorescence (data not shown).

glu-plg (Fig. 3B) also induced an increase in the relative intrinsic fluorescence of glu-plg ($\Delta F=785$) which was suggestive of a conformational change.

Extrinsic fluorescence spectroscopy

The disadvantage of using the intrinsic fluorescence method is that higher concentrations of α -enolase than those used in Figure 3 contributed to the intrinsic fluorescence of the system (data not shown). Therefore, reliable titration curves could not be obtained. To overcome this problem, the change in fluorescence associated with

FITC-labelled glu-plg was measured in the presence of various concentrations of α -enolase (Fig. 4C). In addition, various concentrations of two other plg binding ligands namely, tranexamic acid and poly-D-lysine were also used for comparison (Figs 4A & B). All of the ligands increased the fluorescence of FITC-glu-plg such that the maximal ligand-induced change was between 7 and 10% of the total fluorescence of FITC-glu-plg ($\Delta/F\%$; Fig. 4). These were comparable in magnitude to the reported fluorescence changes induced by small lysine analogues on glu-plg.¹⁹ The maximal fluorescence changes in FITC-glu-plg were induced by molar excesses of ligand. For example, molar ratios of greater than 5 : 1 of α -enolase to FITC-glu-plg (i.e. greater than $20 \mu\text{g/ml}$ of α -enolase) were required to approach maximal fluorescence changes (Fig. 4C). These fluorescence data suggest that α -enolase can induce a conformational change in glu-plg thereby confirming Reaction scheme 3 as a viable model for the binding of glu-plg to α -enolase.

Hill plots were utilized to determine the type of conformational change that these ligands induced in FITC-glu-plg. The slope of the Hill plot (Fig. 4A, inset) that describes the binding of tranexamic acid to FITC-glu-plg, was approximately 1.5. This result confirmed the observations of Christensen and Molgaard,¹⁹ that the binding of tranexamic acid to glu-plg is associated with a cooperative conformational change. Similarly, the interaction of poly-D-lysine with FITC-glu-plg resulted in a Hill coefficient greater than 1 (i.e. approximately 1.5; Fig. 4B, inset) suggesting that glu-plg binds cooperatively to poly-D-lysine. The binding of FITC-glu-plg to α -enolase resulted in a Hill coefficient of 1.02 (Fig. 4C, inset) suggesting that the interaction was not a cooperative process.

DISCUSSION

This study aimed to define the type of binding kinetics and associated conformational changes glu-plg undergoes when it binds to its cellular receptor, α -enolase. Experiments were performed using BIAcore technology under physiological-like conditions and analyzed using BIAevaluation software (version 3.0). Identical experiments were performed with lys-plg for direct comparison with glu-plg on the basis that lys-plg has a more open conformation and is more readily activated.^{10,31} This is a feature of lys-plg exploited in numerous studies that have compared conformational status with the activation of the different plgs, both in solution and in the presence of binding moieties (reviewed in 31), as well as with their binding parameters.

The simplest reaction model describing the lysine-dependent dissociation phases of both the glu- and lys-plg sensorgrams is the non-linear multiple component dissociation model (Reaction scheme 2). Glu-plg has also

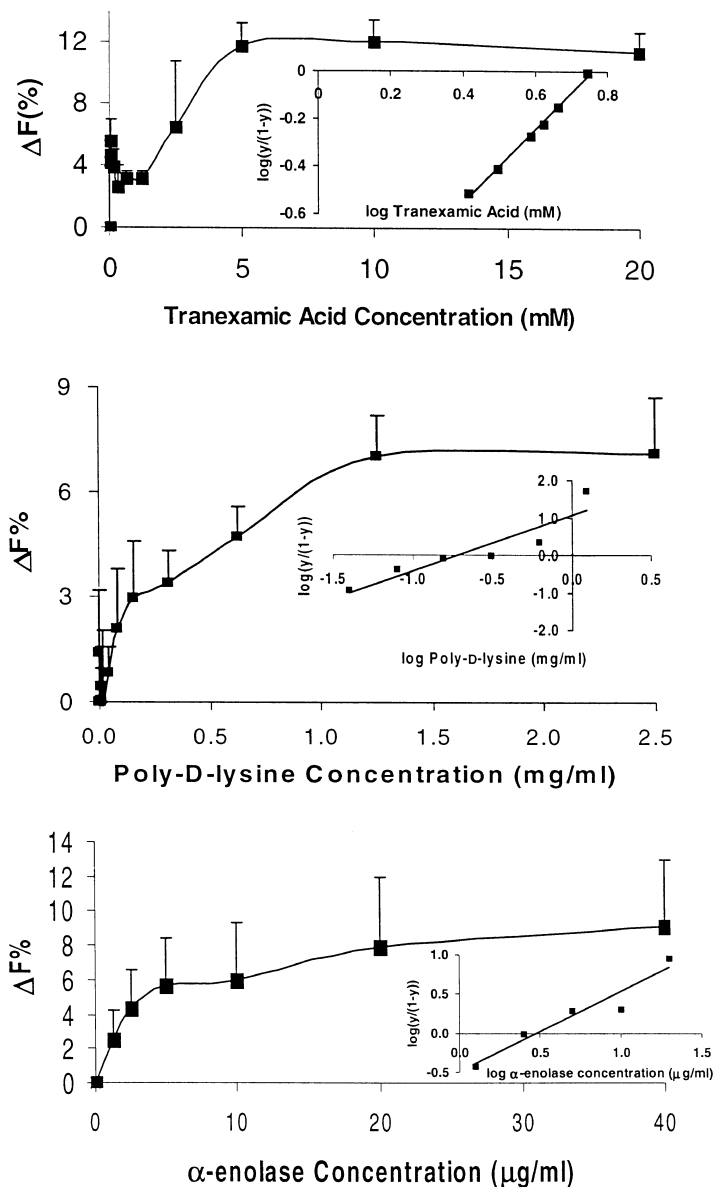


Fig. 4 Normalized fluorescence emission intensities ($\Delta F\%$) obtained after the interaction of FITC-glu-plg with various concentrations of (A) tranexamic acid, (B) poly-D-lysine and (C) α -enolase, plotted against the concentrations of these ligands. The inset shows a Hill plot for each of the ligands. The fractional saturation (y) is defined as: $(F_1 - F)/(F_1 - F_i)$, where F_1 is the initial fluorescence of FITC-glu-plg in the absence of ligand, F_1 is the fluorescence of FITC-glu-plg at the maximal ligand concentration used and F is the fluorescence associated with a specific concentration of ligand.

been shown to bind to a lysine-derivitized sensor chip surface with multiple dissociation reactions.³² Such multiple dissociation reactions were not surprising since both plg species have four functional LBSs that are potentially available for binding. The contours of the sensorgrams, being obviously different, were suggestive of different binding mechanisms, as might also have been expected from the different initial conformations of glu- and lys-plg. Global fitting of the glu-plg binding data was accurately described by the two state reaction/conformational

change model (Reaction scheme 3) over the entire concentration range of glu-plg used (which spanned its physiological concentration of 2 μ M), whereas the lys-plg binding data was not. In fact, lys-plg was not adequately described by any of the currently available global fitting algorithms, at least under the physiological conditions we used to compare glu- and lys-plg binding.

The two-state reaction/conformational change model that describes the binding of glu-plg to α -enolase suggests that the initial conformation of glu-plg is altered

after it has been bound by α -enolase. In a manner similar to tranexamic acid or poly-D-lysine, α -enolase produced a concentration-dependent increase in the fluorescence of FITC-glu-plg. An increase in the intrinsic fluorescence of glu-plg, induced by lysine analogues, is associated with an open conformation of glu-plg,¹⁹ an observation we made with α -enolase. This suggested that α -enolase induces a lysine-dependent conformational change in glu-plg to a more open form. Taken together, these fluorescence studies validate the two-state reaction/conformational change model as a description of the binding of glu-plg to α -enolase.

The association phase kinetics of glu-plg binding to α -enolase suggested by the two-state conformational change model are complex. The relative magnitudes of k_{a1} and k_{a2} for this interaction differ by approximately six orders of magnitude, indicating that the majority of the observed binding of glu-plg to α -enolase is characterized by the initial binding reaction. However, k_{a1} , unlike k_{a2} , increases with decreasing glu-plg concentrations. A decreasing concentration of glu-plg can also be viewed as a relative increase in the α -enolase abundance which is paralleled by an increase in k_{a1} . The acceleration in the initial glu-plg to α -enolase binding rate as the relative concentration of α -enolase increases would indicate a competition reaction. This suggests that during the initial interaction, an α -enolase lysine residue competes with and displaces a lysine residue of glu-plg from one of its LBS motifs. This would disrupt the closed, lysine-dependent conformation of glu-plg and induce a conformational change in the zymogen. The second binding event (k_{a2}) may stabilize this new conformation of glu-plg.

The conformational change of FITC-glu-plg induced by both tranexamic acid and poly-D-lysine, was co-operative. In contrast, the binding of glu-plg to α -enolase was not co-operative (as opposed to non-co-operative). This suggests that the multiple kringle LBSs that bind to the lysine residues of α -enolase induce a conformational change to glu-plg independent of each other. Hence, the interaction of glu-plg with α -enolase would be mediated by at least two binding events; an initial competition reaction followed by a second binding event. As a result of these interactions, glu-plg changes conformation to a more open form, which is stabilized by a second binding event (slower dissociation rate). The actual lysine residues of α -enolase(s) involved in the interaction with glu-plg remain to be determined. There are several possible candidates of which the C-terminal lysine is likely to play a role.^{27,28}

Taken together, our data suggest that at circulating levels of 2 μ M, glu-plg will bind to cell surface receptors (such as α -enolase) and be converted to an open conformation. This finding agrees with the well-documented observation that binding of small lysine analogues to

glu-plg changes its conformation,^{10,12,14,15,18,19,21} which in turn enhances its activation rate by the plg activators.^{14,15,21-23} In addition, it has been shown that the lysine-dependent binding of glu-plg to fibrin,^{24,34} cells^{26,33-36} and isolated receptors^{33,37,38} including α -enolase,^{27,28} facilitates an increase in the rate of glu-plg activation. Since the interaction between glu-plg and α -enolase is associated with a change to a more open conformation of glu-plg, it is suggested that the physiologically important role of cell-surface plg binding proteins³⁹ is to present glu-plg in a form that is essential for its efficient activation by the plg activators.

ACKNOWLEDGMENTS

We thank Rick Filonzi from BIACORE AB for kindly providing the NTA sensor chip used in this study. The order of authorship on this manuscript is alphabetical and does not reflect the relative contribution each author made to the manuscript. NMA was funded in part by an American Diagnostica-University of Wollongong PhD scholarship obtained by MSB from American Diagnostica Inc., Greenwich, CT, USA., and by project grant #970808 obtained by MR from the National Health and Medical Research Council of Australia. This study was also supported in part by project grant #940857 (MSB) from the National Health and Medical Research Council of Australia.

REFERENCES

- Pollanen J, Stephens RW, Vaheri A. Directed plasminogen activation at the surface of normal and malignant cells. *Adv Cancer Res* 1991; 57: 273-328.
- Mathews II, Vanderhoff-Hanaver P, Castellino FJ, Tulinsky A. The crystal structures of the recombinant kringle 1 domain of human plasminogen in complexes with the 3 ligands, ϵ -aminocaproic acid and 4 trans-4-aminomethylcyclohexane-1-carboxylic acid). *Biochemistry* 1996; 35: 2567-2576.
- Mulichak AM, Tulinsky A, Ravichandra KG. Crystal and molecular structure of human plasminogen kringle 4 refined at 1.9-Å resolution. *Biochemistry* 1991; 30: 10576-10588.
- Wu T-P, Padmana Bhanbhan K, Tulinsky A, Mulichak AM. The refined structure of ϵ -aminocaproic acid complexed human plasminogen kringle 4. *Biochemistry* 1991; 30: 10589-10594.
- Chang Y, Mochalkin I, McCance SG, Cheng B, Tulinsky A, Castellino FJ. Structure and ligand binding determinants of the recombinant kringle 5 domain of human plasminogen. *Biochemistry* 1998; 37: 3258-3271.
- Tranqui L, Prandini M, Chapel A. The structure of plasminogen studied by electron microscopy. *Biol Cellulaire* 1979; 34: 39-42.
- Ponting CP, Holland SK, Cederholm-Williams SA, Marshall JM, Brown AJ, Spraggon G, Blake CCF. The compact domain conformation of human glu-plasminogen in solution. *Biochim Biophys Acta* 1992; 1159: 155-161.
- Mangel WF, Lin B, Ramakrishnan V. Characterisation of an extremely large, ligand-induced conformational change in plasminogen. *Science* 1990; 248: 69-73.

9. Summaria L, Arzadon L, Bernabe P. Characterisation of the NH₂-terminal glutamic acid and NH₂-terminal lysine forms of plasminogen isolated by affinity chromatography and isoelectric focusing methods. *J Biol Chem* 1973; 248: 2984–2991.
10. Marshall JM, Brown AJ, Ponting CP. Conformational studies of human plasminogen and plasminogen fragments: evidence for a novel third conformation of plasminogen. *Biochemistry* 1994; 33: 3599–3606.
11. Weisel JW, Nagaswami C, Korsholm B, Petersen LC, Suenson E. Interactions of plasminogen with polymerizing fibrin and its derivatives, monitored with a photoaffinity cross-linker and electron microscopy. *J Mol Biol* 1994; 235: 1117–1135.
12. McCance SG, Castellino FJ. Contributions of the individual kringle domains toward maintenance of the chloride-induced tight conformation of human glutamic acid-1 plasminogen. *Biochemistry* 1995; 34: 9581–9586.
13. Cockell CS, Marshall JM, Dawson KM, Cederholm-Williams. Evidence that the conformation of unliganded human glu-plasminogen is maintained via an intramolecular interaction between the lysine-binding site of kringle 5 and the N-terminal peptide. *Biochem J* 1998; 333: 99–105.
14. Markus G, Priore RL, Wissler FC. The binding of tranexamic acid to native (Glu) and modified (lys) human plasminogen and its effect on conformation. *J Biol Chem* 1979; 254: 1211–1216.
15. Markus G, DePasquale JL, Wissler FC. Quantitative determination of the binding of ϵ -aminocaproic acid to native plasminogen. *J Biol Chem* 1978; 253: 727–732.
16. Sjöholm I, Wiman B, Wallen P. Studies of the conformation changes of plasminogen during activation to plasmin and by 6-aminohexanoic acid. *Eur J Biochem* 1973; 39: 471–479.
17. Ramakrishnan V, Patthy L, Mangel WF. Conformation of Lys-plasminogen and the kringle 1–3 fragment of plasminogen analysed by small-angle neutron scattering. *Biochemistry* 1991; 30: 3963–3969.
18. Christensen U, Molgaard L. Stopped-flow kinetic studies of glu-plasminogen. Conformational changes triggered by AH-site ligand binding. *FEBS Lett* 1991; 278: 204–206.
19. Christensen U, Molgaard L. Stopped-flow kinetic studies of glu-plasminogen. Conformational changes triggered by AH-site ligand binding. *Biochem J* 1992; 285: 419–425.
20. Varadi A, Patthy L. Kringle 5 of human plasminogen carries a benzamidine-binding site. *Biochem Biophys Res Commun* 1981; 103: 97–102.
21. Banyai L, Patthy L. Proximity of the catalytic region and the kringle 2 domain in the closed conformer of plasminogen. *Biochim Biophys Acta* 1985; 832: 224–227.
22. Lucas MA, Straight DL, Fretto LJ, McKee PA. The effects of fibrinogen and its cleavage products on the kinetics of plasminogen activation by urokinase and subsequent plasmin activity. *J Biol Chem* 1983; 258: 12171–12177.
23. Peltz SW, Hardt TA, Mangel WF. Positive regulation of plasminogen by urokinase: differences in the K_m for (glutamic acid) plasminogen and lysine-plasminogen and effect of certain α,ω -amino acids. *Biochemistry* 1982; 21: 2798–2804.
24. Ranby M. Studies in the kinetics of plasminogen activation by tissue plasminogen activator. *Biochim Biophys Acta* 1982; 704: 461–469.
25. Plow EF, Herren T, Redlitz A, Miles LA, Hoover-Plow JL. The cell biology of the plasminogen system. *FASEB J* 1995; 9: 939–945.
26. Ranson M, Andronicos NM, O'Mullane MJ, Baker MS. Increased plasminogen binding is associated with metastatic breast cancer cells: differential expression of plasminogen binding proteins. *Br J Cancer* 1998; 77: 1586–1597.
27. Andronicos NM, Ranson M, Bognacki J, Baker MS. The human ENO1 gene product (recombinant human α -enolase) displays characteristics required for a plasminogen binding protein. *Biochim Biophys Acta* 1997; 1337: 27–39.
28. Redlitz A, Fowler BJ, Plow EF, Miles LA. The role of an enolase-related molecule in plasminogen binding to cells. *Eur J Biochem* 1995; 227: 407–415.
29. Nice EC, Mcinerney TL, Jackson, DC. Analysis of the interaction between a synthetic peptide of influenza virus hemagglutinin and monoclonal antibody using an optical biosensor. *Mol Immunol* 1996; 33: 659–670.
30. Lackmann M, Mann RJ, Kravets L et al. Ligand for EpH-related kinase (LERK) 7 is the preferred high affinity ligand for the HEK receptor. *J Biol Chem* 1997; 272: 16521–16530.
31. Markus G. Conformational changes in plasminogen, their effect on activation and the agents that modulate activation rates—a review. *Fibrinolysis* 1996; 10: 75–85.
32. Warkentin PH, Johansen K, Brash JL, Lundstrom I. The kinetics and affinity of binding of glu-plasminogen specific to the ϵ -amino group of L-lysine: its potential application to modified biomaterials. *J Coll Inter Sci* 1998; 199: 131–139.
33. Borza D-B, Morgan WT. Acceleration of plasminogen activation by tissue-plasminogen activator on surface bound histidine-rich glycoprotein. *J Biol Chem* 1997; 272: 5718–5726.
34. Felez J, Miles LA, Fabregas P, Jardi M, Plow EF, Lijnen RH. Characterisation of cellular binding sites and interactive regions within reactants required for enhancement of plasminogen activation by tPA on the surface of leucocytic cells. *Thromb Haemost* 1996; 76: 25684–25691.
35. Pernod G, Aouffen M, Polack B, LeMagueresse B, Benabid AL, Kolodie L. tPA-dependent activation of C6 glioma-bound plasminogen: a kinetic study. *Fibrinol Proteol* 1998; 12: 137–144.
36. Hajjar KA, Hamel NM, Harpel PC, Nuchman RL. Binding of tissue plasminogen activator to cultured human endothelial cells. *J Clin Invest* 1987; 80: 1712–1719.
37. Cesarman GM, Guevara CA, Hajjar KA. An endothelial cell receptor for plasminogen/tissue plasminogen activator (t-PA). II. Annexin II-mediated enhancement of tPA-dependent plasminogen activation. *J Biol Chem* 1994; 269: 21198–21203.
38. Lind SE, Smith CJ. Actin accelerates plasmin generation by tissue plasminogen activator. *J Biol Chem* 1991; 266: 17673–17678.
39. Namiranian S, Naito Y, Kakkar VV, Scully MF. Bound plasminogen is rate-limiting for cell-surface-mediated activation of plasminogen by urokinase. *Biochem J* 1995; 309: 977–982.